

# Generalizing continuous flexible Kokotsakis belts of the isogonal type\*

Georg Nawratil<sup>[0000–0001–8639–9064]</sup>

Institute of Discrete Mathematics and Geometry &  
Center for Geometry and Computational Design,  
TU Wien, Austria, [nawratil@geometrie.tuwien.ac.at](mailto:nawratil@geometrie.tuwien.ac.at)  
<https://www.geometrie.tuwien.ac.at/nawratil/>

**Abstract.** Kokotsakis studied the following problem in 1932: Given is a rigid closed polygonal line (planar or non-planar), which is surrounded by a polyhedral strip, where at each polygon vertex three faces meet. Determine the geometries of these closed strips with a continuous mobility. On the one side, we generalize this problem by allowing the faces, which are adjacent to polygon line-segments, to be skew; i.e. to be non-planar. But on the other side, we restrict to the case where the four angles associated with each polygon vertex fulfill the so-called isogonality condition that both pairs of opposite angles are equal or supplementary. In more detail, we study the case where the polygonal line is a skew quad, as this corresponds to a  $(3 \times 3)$  building block of a so-called V-hedra composed of skew quads. The latter also gives a positive answer to a question posed by Robert Sauer in his book of 1970 whether continuous flexible skew quad surfaces exist.

**Keywords:** Kokotsakis belt · continuous flexibility · skew quad surfaces.

## 1 Introduction

Let us consider a so-called Kokotsakis belt as described in [1], which is illustrated in Fig. 1a. In general these loop structures are rigid, thus continuous flexible ones possess a so-called overconstrained mobility. Kokotsakis himself formulated the problem for general rigid closed polygonal lines  $p$ , but in fact he only studied flexible belts with planar polygons  $p$  in [1]. Planarity was only not assumed in the study of necessary and sufficient conditions for infinitesimal flexibility (see also Karpenkov [2]). Clearly, the restriction to planar polygons  $p$  makes sense in the context of continuous flexible polyhedra, as this condition has to be fulfilled around faces where all vertices have valence four<sup>1</sup>.

Our interest in Kokotsakis belts results from our research on continuous flexible polyhedral surfaces; especially those composed of rigid planar quads in the combinatorics of a square grid. A very well known class of these flexible planar-quad (PQ) surfaces are *V-hedra*, which are the discrete analogs of Voss surfaces<sup>2</sup> according to [4].

\*Dedicated to my newborn son and his mother on the occasion of his birth.

<sup>1</sup>Assumed that this part of the continuous flexible polyhedra is not rigid.

<sup>2</sup>Surfaces on which geodesic lines form a conjugate curve network [3].

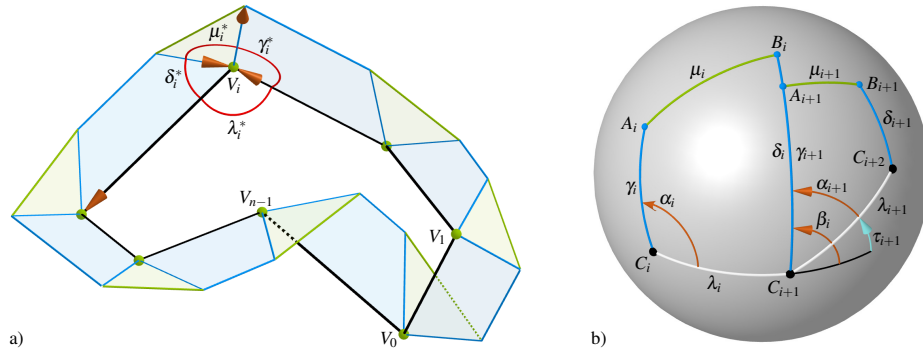


**Fig. 1.** Original Kokotsakis belt: (a) A rigid closed polygonal line  $p$  (not necessarily planar) with  $n$  vertices  $V_0, \dots, V_{n-1}$  is surrounded by a belt of planar polygons in a way that each vertex  $V_i$  of  $p$  has valence four. Moreover, the planar angles  $\delta_i^*, \gamma_i^*, \lambda_i^*, \mu_i^* \in (0; \pi)$  are illustrated as well as the orientation of the enclosing line-segments used for the construction of the spherical image, which is illustrated in parts in (b). Note that the edge  $V_{i-1}V_i$  is mapped to the point  $C_i$ .

They can easily be characterized by the fact that in each vertex the angles of opposite planar quads are equal. The question whether V-hedra can be generalized by dropping the planarity condition of the quads (cf. Fig. 2) motivated us for the study at hand, which is structured as follows: We proceed in Section 1.1 with a literature review on flexible Kokotsakis belts, where we place emphasis on the so-called isogonal type<sup>3</sup>, which means that in every polygon vertex both pairs of opposite angles are (1) equal or (2) supplementary. In Section 2 we discuss the spherical image of Kokotsakis belts from a kinematical point of view. Based on these consideration we study generalized flexible Kokotsakis belts of the isogonal type in Section 3. In Section 4 we discuss continuous flexible skew-quad (SQ) surfaces, where we focus on V-hedra composed of skew quads in more detail. The paper is concluded in Section 5.

### 1.1 Review on continuous flexible Kokotsakis belts

Until now only examples of continuous flexible Kokotsakis belts are known where the rigid polygon line  $p$  is planar as well as all faces adjacent to its line-segments. Therefore these assumptions hold for the complete review section, which is structured along the number  $n$  of vertices  $V_0, \dots, V_{n-1}$  of  $p$  (cf. Fig. 1a).

General results were only obtained by Kokotsakis [1] for the isogonal type, to which for example rigidly foldable origami twists [5] belong as a special case. For  $n = 3$  and  $n = 4$  more results are known, which can be summarized as follows:

- **Case  $n = 3$ :** This case implies continuous flexible octahedra, which are very well studied objects dating back to Bricard [7]. Especially, the Bricard octahedra of the 3rd type (cf. [8]) correspond to the isogonal case, which was already pointed out by Kokotsakis [1]. Moreover, the study of these Kokotsakis belts allows also the determination of continuous flexible octahedra with vertices at infinity [9].

<sup>3</sup>This notation is in accordance with [6].

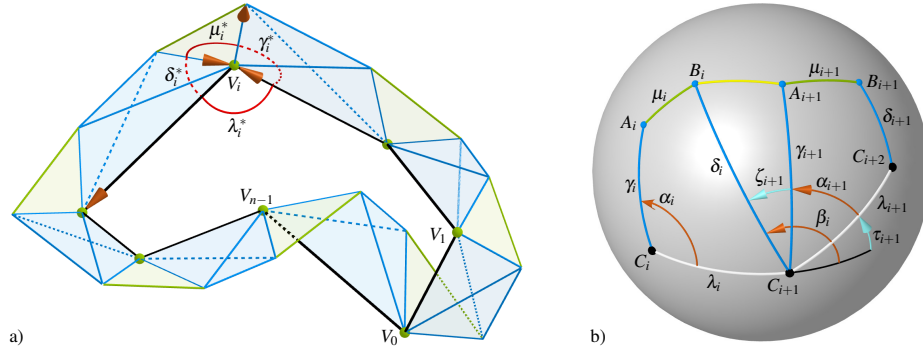


**Fig. 2.** Generalized Kokotsakis belt: (a) It is obtained from the original Kokotsakis belt illustrated in Fig. 1 by dropping the planarity condition of the faces adjacent to the polygon line-segments of  $p$ . The resulting spatial structures are illustrated as tetrahedra. A part of the corresponding spherical image of the generalized Kokotsakis belt is visualized in (b).

- **Case  $n = 4$ :** These Kokotsakis belts, which are also known as  $(3 \times 3)$  complexes, are the building blocks of continuous flexible PQ surfaces according to [4, Theorem 3.2]. Based on spherical kinematic geometry [6], a partial classification of continuous flexible  $(3 \times 3)$  building blocks was obtained by Stachel and the author [10,11,12]. Inspired by this approach, Izmistiev [13] obtained a full classification containing more than 20 cases.

Note that the first classes of continuous flexible PQ surfaces were given by Sauer and Graf [14]; namely the so-called T-hedra (see also [15,16]) and the already mentioned V-hedra (see also [15,17]).

A rigid-foldable PQ surface which can be developed is a special case of origami. Under the additional condition of flat-foldability (as in case of the popular Miura-ori) Tachi [18,19] developed computational tools to design surfaces, where each vertex is of the isogonal type. Recently, Feng et al. [20] gave a complete analysis of the flat-foldable case, which can also be used for design tasks [21].

Within the field of computational design Jiang et al. [22] presented recently an optimization technique to penalize an isometrically deformed surface with planar quads. Its design space is restricted to rigid-foldable quad-surfaces which can be seen as a discretization of flexible smooth surfaces (e.g. Voss surfaces, profile-affine surfaces [14,15]).

## 2 Spherical image of Kokotsakis belts

In order to get a consistent notation for the construction of the spherical image of the Kokotsakis belt we orient the line-segments meeting at a vertex  $V_i$  according to Figs. 1a and 2a, respectively. Taking this orientation of the line-segments into account, the spherical 4-bar mechanism, which corresponds with the arrangement of faces around  $V_i$ , has the following spherical bar lengths:

$$\delta_i = \pi - \delta_i^*, \quad \gamma_i = \pi - \gamma_i^*, \quad \lambda_i = \pi - \lambda_i^*, \quad \mu_i = \pi - \mu_i^* \quad (1)$$

for the index<sup>4</sup>  $i = 0, \dots, n-1$ . The spherical image of faces around two adjacent vertices  $V_i$  and  $V_{i+1}$  is illustrated in Figs. 1b and 2b, which show the motion transmission from the vertex  $C_i$  over  $C_{i+1}$  to  $C_{i+2}$  by two coupled spherical 4-bar mechanisms. Note that in the isogonal case these 4-bar mechanisms are so-called spherical isograms fulfilling one of the following two conditions:

$$(1) \quad \lambda_i = \mu_i, \quad \delta_i = \gamma_i, \quad (2) \quad \lambda_i + \mu_i = \pi, \quad \delta_i + \gamma_i = \pi. \quad (2)$$

Note that these two types are related by the replacement of one of the vertices of the spherical isogram by its antipodal point, which does not change its motion. In Section 3 we show that we can restrict to type (1) without loss of generality by assuming an appropriate choice of orientations. In the following we use the half-angle substitutions

$$\sin \alpha_i = \frac{2a_i}{1+a_i^2}, \quad \cos \alpha_i = \frac{1-a_i^2}{1+a_i^2}, \quad \sin \beta_i = \frac{2b_i}{1+b_i^2}, \quad \cos \beta_i = \frac{1-b_i^2}{1+b_i^2}, \quad (3)$$

in order to end up with algebraic expressions. It is well known (e.g. [6]) that the input angle  $\alpha_i$  and the output angle  $\beta_i$  of the  $i$ -th spherical isogram of type (1) of Eq. (2) are related by

$$b_i = f_i a_i \quad \text{with} \quad f_i \neq 0 \quad \text{and} \quad f_i = \frac{\sin \delta_i \pm \sin \lambda_i}{\sin(\delta_i - \lambda_i)}. \quad (4)$$

The two options in the expression for  $f_i$  implied by the  $\pm$  sign refer to the case whether the motion transmission corresponds to that of a spherical parallelogram ( $\Leftrightarrow f_i > 0$ ) or spherical antiparallelogram ( $\Leftrightarrow f_i < 0$ ), respectively. Note that the degenerated cases ( $\delta_i = \lambda_i$  and  $\delta_i + \lambda_i = \pi$ ) of the spherical isogram are excluded by the condition  $f_i \neq 0$  given in Eq. (4).

The angles  $\beta_i$  and  $\alpha_{i+1}$  are related over the offset angle  $\varepsilon_{i+1}$ ; i.e.  $\beta_i + \varepsilon_{i+1} = \alpha_{i+1}$ . This means that  $\varepsilon_{i+1}$  gives only the shift between the output angle  $\beta_i$  of the  $i$ -th isogram to the input angle  $\alpha_{i+1}$  of the  $(i+1)$ -th isogram. This yields the relation:

$$\tan \alpha_{i+1} = \frac{\tan \beta_i + \tan \varepsilon_{i+1}}{1 - \tan \beta_i \tan \varepsilon_{i+1}}. \quad (5)$$

Using the half-angles and the Weierstrass substitution  $e_{i+1} := \tan \frac{\varepsilon_{i+1}}{2}$  yield

$$a_{i+1} = \frac{b_i + e_{i+1}}{1 - b_i e_{i+1}}. \quad (6)$$

Note that the spherical arcs  $B_i C_{i,i+1}$  and  $A_{i+1} C_{i,i+1}$  enclose the angle  $\zeta_{i+1} := \varepsilon_{i+1} + \tau_{i+1}$  (cf. Fig. 2b), where the latter angle is the torsion angle of the spatial polygon  $\mathfrak{p}$ , which is defined as the angle enclosed by the spherical arcs  $C_i C_{i+1}$  and  $C_{i+1} C_{i+2}$ . From the polygon  $\mathfrak{p}$  the angles  $\tau_{i+1}$  can be computed as the angle of rotation about the oriented axis  $V_i V_{i+1}$ , which brings the plane  $[V_{i-1}, V_i, V_{i+1}]$  to the plane  $[V_i, V_{i+1}, V_{i+2}]$ . Therefore  $\tau_{i+1}$ , which is within the interval  $(-\pi; \pi]$ , can be computed as:

$$\tau_{i+1} = \text{sign}(o) \arccos \left( \frac{(c_i \times c_{i+1}) \cdot (c_{i+1} \times c_{i+2})}{\|c_i \times c_{i+1}\| \|c_{i+1} \times c_{i+2}\|} \right) \quad \text{with} \quad o := (c_i \times c_{i+1}) \cdot c_{i+2} \quad (7)$$

where  $c_i$  denotes the vector from  $V_{i-1}$  to  $V_i$ .

*Remark 1.* For the original Kokotsakis belt (cf. Fig. 1) the angle  $\zeta_{i+1}$  is zero ( $\Rightarrow \varepsilon_{i+1} = -\tau_{i+1}$ ) or  $\pi$  ( $\Rightarrow \varepsilon_{i+1} = \pi - \tau_{i+1}$ ) for all  $i = 0, \dots, n-1$ . Note that  $\mathfrak{p}$  is a planar curve if all  $\tau_{i+1}$  are either zero or  $\pi$ .  $\diamond$

<sup>4</sup>Note that in the remainder of the paper the indices are taken modulo  $n$ .

### 3 Continuous flexible Kokotsakis belts of the isogonal type

According to [6, Theorem 1] the Kokotsakis belt is continuous flexible if and only if the spherical image has this property. Now we will show that any Kokotsakis belt of the isogonal type can be identified with a spherical mechanism, which is only composed of spherical isograms of type (1) in Eq. (2):

We start with the spherical image of  $p$ , i.e. the points  $C_0, \dots, C_{n-1}$  and construct the spherical points  $A_0$  and  $B_0$  according to Section 2. If the spherical isogram  $C_0C_1B_0A_0$  is of type (2) then we replace  $B_0$  by its antipode. Then we proceed as follows around the spherical image of the polyline  $p$ ; i.e. for  $i = 0, \dots, n-1$ :

- a. In the case where the two antipodal points, which are candidates for  $A_{i+1}$ , correspond with the values zero and  $\pi$  for  $\varepsilon_{i+1}$ , we have to choose the one which implies  $\varepsilon_{i+1} = 0$  as  $\varepsilon_{i+1} = \pi$  is not covered by Eq. (6). In any other case  $A_{i+1}$  can be chosen arbitrary from the corresponding set of two antipodal points.
- b.  $B_{i+1}$  has to be chosen from the corresponding set of two antipodal points such that the spherical isogram  $C_{i+1}C_{i+2}B_{i+1}A_{i+1}$  is of type (1).

We can end up in two situations; either  $A_n = A_0$  and we are done or  $A_n$  is the antipodal point of  $A_0$ . In the latter case we denote by  $j$  the highest possible index within the set  $\{0, \dots, n-1\}$  for which the choice of  $A_{i+1}$  was done arbitrarily in step (a). Then we replace all  $A_{i+1}$  and  $B_{i+1}$  with  $i \geq j$  by their antipodal points which yields  $A_n = A_0$ .

Note that such a  $j$  has to exist as otherwise we can construct the following contradiction: No  $j$  exists if and only if there are no shifts; i.e.  $e_0 = e_1 = \dots = e_{n-1} = 0$ . As a consequence  $\alpha_0 = \beta_0 = 0$  implies  $\alpha_{i+1} = \beta_{i+1} = 0$  for all  $i \in \{0, \dots, n-1\}$ , which already shows that in this case  $A_n = A_0$  has to hold.

As a consequence of the above considerations one can write down the condition for continuous flexibility of any Kokotsakis belt of the isogonal type, where the rigid polygon  $p$  has  $n > 2$  vertices, as

$$a_0 - a_n = 0. \quad (8)$$

In this so-called closure condition we substitute  $a_n$  by

$$a_i = \frac{a_{i-1}f_{i-1} + e_i}{1 - a_{i-1}f_{i-1}e_i} \quad (9)$$

which results from Eq. (6) under consideration of Eq. (4). By iterating this substitution (in total  $n$  times) we end up with an expression of the form  $q_2 a_0^2 + q_1 a_0 + q_0 = 0$  where  $q_2, q_1, q_0$  are functions in  $f_0, \dots, f_{n-1}, e_0, \dots, e_{n-1}$ . This means that the spherical coupler arms  $A_0C_0$  and  $A_nC_0$  coincide for all input angles  $\alpha_0$  if and only if the following necessary and sufficient conditions for continuous mobility are fulfilled:

$$q_2 = 0, \quad q_1 = 0, \quad q_0 = 0. \quad (10)$$

This results in the following theorem:

**Theorem 1.** *For a given polyhedral curve  $p$  with  $n$  vertices, there exists at least a  $(2n - 3)$ -dimensional set of continuous flexible Kokotsakis belts of the isogonal type over  $\mathbb{C}$ .*

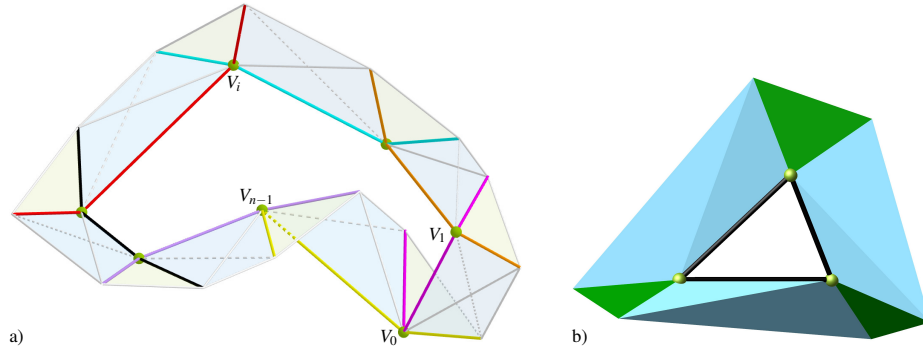


**Fig. 3.** Generalized Kokotsakis belt of the isogonal type: (a) Edges with the same absolute values of their rotation angles during the continuous flexibility are illustrated with the same color. (b) For  $n = 3$  we obtain an overconstrained angle-symmetric 6R linkage.

By taking a closer look at  $q_2 = 0$  it can easily be seen that the terms linear in  $e_i$  are given by  $f_0 e_1$  and  $f_0 \dots f_{k-1} e_k$  for  $k = 2, \dots, n$ . In the equation  $q_0 = 0$  the linear terms in  $e_i$  are  $e_0$ ,  $e_{n-1} f_{n-1}$  and  $e_k f_k \dots f_{n-1}$  for  $k = 1, \dots, n-2$ . Therefore each of the two conditions  $q_2 = 0$  and  $q_0 = 0$  can only be fulfilled independently from the choice of the  $f_i$ 's if there are no shifts; i.e.  $e_0 = e_1 = \dots = e_{n-1} = 0$ . Note that these are not only necessary conditions but already sufficient ones as they imply  $q_2 = q_0 = 0$ . In this case the remaining condition  $q_1 = 0$  simplifies to  $f_0 f_1 \dots f_{n-1} = 1$  and we end up with a  $(n-1)$ -dimensional set of continuous flexible Kokotsakis belts of the isogonal type over  $\mathbb{C}$ . Note that  $e_0 = e_1 = \dots = e_{n-1} = 0$  only implies planarity of  $p$  if we assume the faces to be planar.

For a spatial polyline  $p$  with planar faces the spherical coupler arms  $B_i C_{i+1}$  and  $A_{i+1} C_{i+1}$  are aligned. Therefore all  $e_{i+1}$  are determined (cf. Remark 1) and we get:

**Theorem 2.** *For a given polyhedral curve  $p$  with  $n > 3$  vertices, there exists at least a  $(n-3)$ -dimensional set of continuous flexible Kokotsakis belts with planar faces of the isogonal type over  $\mathbb{C}$ . For planar curves  $p$  (which is always true for  $n = 3$ ) this dimension raises to  $(n-1)$ .*

### 3.1 Property regarding the rotation angles

According to [1, §8] opposite angles in a spherical isogram are either equal or complete each other to  $2\pi$ . As a consequence opposite dihedral angles along edges meeting in a vertex  $V_i$  have at each time instant  $t$  the same absolute value of their angular velocities. Therefore the absolute values of the rotation angles around these two edges are the same (measured from an initial starting configuration). As one of the dihedral angles is the angle about an edge  $V_i V_{i+1}$  of the polygon  $p$ , this property holds for the two spherical 4-bars, which have the common point  $C_{i+1}$  (cf. Figs. 1b and 2b, respectively). Therefore the same absolute values of the rotation angle can always be assigned to three edges within a continuous flexible Kokotsakis belt of the isogonal type (cf. Fig. 3a).

*Example 1.* Now we consider the case  $n = 3$ . For any choice of  $\delta_i$  and  $\gamma_i$  for  $i = 1, 2, 3$  and  $\gamma_1 + \gamma_2 + \gamma_3 = 2\pi$  (closure condition of central triangle) there exist  $e_0, e_1, e_2 \in \mathbb{C}$  such that we get a continuous flexible Kokotsakis belt of the isogonal type. The resulting structure can be seen as an overconstrained 6R loop (cf. Fig. 3b), which belongs to the third class of so-called angle-symmetric 6R linkages [23] due to the above discussed angle property. Note that for  $e_0 = e_1 = e_2 = 0$  we get the already mentioned Bricard octahedron of type III (cf. case  $n = 3$  in Section 1.1).  $\diamond$

## 4 Continuous flexible SQ surfaces

On page 168 of Sauer's book [15] the following open problem is mentioned: *Do there exist continuous flexible SQ surfaces?* We answer this question positively by constructing  $(3 \times 3)$  building blocks of continuous flexible V-hedra with skew quads within this section. The restriction to these substructures is sufficient as Theorem 3.2 of [4] can be generalized in the following way:

**Theorem 3.** *A non-degenerate SQ surface is continuous flexible, if and only if this holds true for every  $(3 \times 3)$  building block.*

*Proof.* The arguments used for the proof of Theorem 3.2 of [4] do not rely on the planarity of the involved quads.  $\square$

### 4.1 Associated overconstrained mechanism

We start this section with the definition of reciprocal-parallel quad meshes:

**Definition 1.** *Two quad meshes  $\mathcal{Q}$  and  $\mathcal{V}$  are called reciprocal-parallel if the following conditions are fulfilled:*

- \*  $\mathcal{Q}$  and  $\mathcal{V}$  are combinatorial dual; i.e. vertices of one mesh correspond to the faces of the other and vice versa.
- \* The edges of both meshes are related by the implied bijection that edges of adjacent face are mapped to edges between corresponding adjacent vertices and vice versa.
- \* Edges, which are related by this bijection, are parallel.

Sauer [15] showed that every infinitesimal flexible quad surface  $\mathcal{Q}$  possesses in general a unique (up to scaling) reciprocal-parallel quad mesh  $\mathcal{V}$  with rigid vertices. The reciprocal-parallel surface of the latter mesh  $\mathcal{V}$  is only uniquely determined (up to scaling) if  $\mathcal{Q}$  is composed of skew quads, otherwise there exist infinitely many, which are in a parallelism relation<sup>5</sup> to each other (cf. [15, Theorem 16.22]).

The corresponding deformation of the  $\mathcal{V}$  mesh during the continuous flexion of  $\mathcal{Q}$  has to be a conformal transformation, as the vertex stars are rigid. The corresponding kinematic structure of  $\mathcal{V}$  is composed of rigid vertex stars linked by cylindrical joints (cf. Fig. 5). Note that in general such a structure only has the trivial mobility resulting from the homothetic transformation. This motion can be omitted by fixing the length of one edge in the structure. These modified linkages are in general rigid but those stemming from continuous flexible quad surfaces  $\mathcal{Q}$  have an overconstrained motion.

<sup>5</sup>Corresponding faces and edges of these meshes are parallel.

#### 4.2 V-hedra with skew quads

We study this class in more detail, as it is a generalization of V-hedra with planar quads having many applications to structural engineering practice [17,24].

For  $n = 4$  the equations  $q_2 = q_1 = q_0 = 0$  of Eq. (10) read as follows:

$$\begin{aligned}
 q_2 &:= f_0[e_0f_3(e_1e_2f_2 + e_2e_3f_1 + e_1e_3 - f_1f_2) + e_1e_2e_3f_2 - e_3f_1f_2 - e_2f_1 - e_1], \\
 q_1 &:= e_1e_2f_0f_2f_3 + e_2e_3f_0f_1f_3 + e_1e_3f_0f_3 - e_1e_3f_1f_2 - f_0f_1f_2f_3 - e_1e_2f_1 \\
 &\quad - e_2e_3f_2 + 1 + e_0(e_1e_2e_3f_1f_3 - e_1e_2e_3f_0f_2 - e_1f_1f_2f_3 + e_3f_0f_1f_2 \\
 &\quad + e_2f_0f_1 - e_2f_2f_3 + e_1f_0 - e_3f_3), \\
 q_0 &:= e_0(e_1e_3f_1f_2 + e_1e_2f_1 + e_2e_3f_2 - 1) + f_3(e_1e_2e_3f_1 - e_1f_1f_2 - e_2f_2 - e_3).
 \end{aligned} \tag{11}$$

We can solve this set of equations explicitly for  $e_1, e_2, e_3$  in dependence of  $e_0, f_0, \dots, f_3$ , which yields the following two solutions:

$$\begin{aligned}
 e_1 &= \frac{e_0f_0f_2(f_1^2-1)(f_3^2-1) \pm R_1R_2}{e_0^2(f_0f_2-f_1f_3)(f_0-f_1f_2f_3) + (f_0f_3-f_1f_2)(f_0f_2f_3-f_1)}, \\
 e_2 &= \frac{\mp R_1R_2}{e_0^2(f_0f_1-f_2f_3)(f_0f_2-f_1f_3) + (f_0f_1f_3-f_2)(f_0f_2f_3-f_1)}, \\
 e_3 &= \frac{e_0f_1f_3(f_0^2-1)(f_2^2-1) \pm R_1R_2}{e_0^2(f_0f_2-f_1f_3)(f_0f_1f_2-f_3) + (f_0f_3-f_1f_2)(f_0f_1f_3-f_2)}
 \end{aligned} \tag{12}$$

with

$$\begin{aligned}
 R_1 &:= \sqrt{e_0^2(f_0f_1-f_2f_3)(f_0f_2-f_1f_3) + (f_0f_1f_3-f_2)(f_0f_2f_3-f_1)}, \\
 R_2 &:= \sqrt{e_0^2(f_0f_1f_2-f_3)(f_1f_2f_3-f_0) + (f_0f_1f_2f_3-1)(f_1f_2-f_0f_3)}.
 \end{aligned} \tag{13}$$

*Remark 2.* Alternatively, the above given equations  $q_2 = q_1 = q_0 = 0$  from Eq. (11) can also be solved explicitly for  $f_1, f_2, f_3$  in dependence of  $f_0, e_0, \dots, e_3$ , which yield the following two solutions:

$$\begin{aligned}
 f_1 &= \frac{-(f_0^2+1)e_0e_1(e_3^2+1)(e_2^2-1) + f_0(e_0^2e_1^2e_2^2 - e_0^2e_1^2e_3^2 - e_0^2e_2^2e_3^2 - e_1^2e_2^2e_3^2 + e_0^2 + e_1^2 + e_2^2 - e_3^2) \pm R_3R_4}{2e_2(e_3^2+1)(e_0f_0+e_1)(e_0e_1-f_0)}, \\
 f_2 &= \frac{(f_0^2+1)e_0e_1(e_3^2+1)(e_2^2+1) - f_0(e_0^2e_1^2e_2^2 + e_0^2e_1^2e_3^2 - e_0^2e_2^2e_3^2 - e_1^2e_2^2e_3^2 - e_0^2 - e_1^2 + e_2^2 + e_3^2) \mp R_3R_4}{2e_2e_3f_0(e_1^2+1)(e_0^2+1)}, \\
 f_3 &= \frac{-(f_0^2+1)e_0e_1(e_3^2-1)(e_2^2+1) - f_0(e_0^2e_1^2e_2^2 - e_0^2e_1^2e_3^2 + e_0^2e_2^2e_3^2 + e_1^2e_2^2e_3^2 - e_0^2 + e_1^2 + e_2^2 - e_3^2) \pm R_3R_4}{2e_3(e_2^2+1)(e_1f_0+e_0)(e_0e_1-f_0)}
 \end{aligned} \tag{14}$$

with

$$\begin{aligned}
 R_{3,4} &:= [f_0(e_0^2e_1^2e_2^2 + e_0^2e_1^2e_3^2 - e_0^2e_2^2e_3^2 - e_1^2e_2^2e_3^2 - e_0^2 - e_1^2 + e_2^2 + e_3^2) \\
 &\quad - (f_0^2+1)e_0e_1(e_3^2+1)(e_2^2+1) \pm 2f_0e_2e_3(e_1^2+1)(e_0^2+1)]^{\frac{1}{2}},
 \end{aligned} \tag{15}$$

where  $R_3$  corresponds to the plus sign and  $R_4$  to the minus sign.  $\diamond$

Note that for a given skew central quad  $p$  and a set of real values  $e_0, \dots, e_3, f_0, \dots, f_3$  fulfilling the three equations  $q_2 = q_1 = q_0 = 0$ , the missing geometric parameters  $\delta_i$  can



be computed from the equation  $\sin \delta_i \pm \sin \lambda_i - f_i \sin (\delta_i - \lambda_i) = 0$  (cf. Eq. (4)). For the minus sign we get one further real solution beside the excluded degenerate case  $\delta_i = \lambda_i$ . By shifting these two values obtained for  $\delta_i$  by  $\pi$  we obtain the solutions of the equation with respect to the plus sign. Therefore we get a unique value for  $\delta_i \in (0; \pi)$  with  $\delta_i \neq \lambda_i$  for each  $i = 0, \dots, 3$ .

*Example 2.* The coordinates of the vertices of the skew central quad  $p$  are given by:

$$V_0 = (5, 0, 0)^T, \quad V_1 = (4, 3, 0)^T, \quad V_2 = (1, 2, 2)^T, \quad V_3 = (0, 0, 0)^T, \quad (16)$$

from which the angles  $\lambda_i$  and  $\tau_i$  for  $i = 0, \dots, 3$  can be calculated. Moreover, the input data is completed by the values:

$$e_0 = 100, \quad d_0 = 0.3, \quad d_1 = 0.15, \quad d_2 = 0.2, \quad d_3 = 0.25, \quad (17)$$

where  $d_i = \tan \frac{\delta_i}{2}$ . From that we can compute the  $f_i$  values according to Eq. (4) with respect to the minus sign for all  $i = 0, \dots, 3$ . Then the formulas for the solution set related to the upper sign in Eq. (12) yield

$$e_1 = -0.86081001, \quad e_2 = -5.06077939, \quad e_3 = 0.57043281. \quad (18)$$

One configuration of the resulting continuous flexible  $(3 \times 3)$  building block of a V-hedra with skew quads is illustrated in Fig. 4, where also the corresponding spherical image is displayed. The associated overconstrained mechanism implied by the reciprocal-parallelism (cf. Section 4.1) is shown in Fig. 5. In the captions of Figs. 4 and 5 we also provide links to gif animations showing the overconstrained motion of these three mechanisms.  $\diamond$

We close this section by making the following two final comments:

- The edges of the V-hedra can be subdivided into two families of discrete parameter lines, which are called  $u$ -polylines and  $v$ -polylines for short. Due to the property pointed out in Section 3.1, the rotation angles along any  $u$ -polyline or  $v$ -polyline are the same. Note that this property is well known for V-hedra with planar quads (cf. [14, page 529]) but also holds for the skew case.
- In view of Section 4.1 it should be noted that there is a further remarkable relation to an overconstrained mechanism beside the one illustrated in Fig. 5. As already pointed out by Sauer [15] the vertex star fulfilling the isogonality condition is reciprocal-parallel to a skew isogram, which has the following additional property: If the four bars of the isogram are hinged in the vertices by rotational joints, which are orthogonal to the plane spanned by the linked bars (cf. Fig. 6), then one obtains a so-called Bennett mechanism [25]. This is the only non-trivial mobile 4R loop. If the quads of the V-hedra  $\mathcal{Q}$  are skew then the four axes of the Bennett mechanisms, which can be associated with a vertex of the mesh  $\mathcal{V}$ , differ from each other (cf. Fig. 6). Only in the case where  $\mathcal{Q}$  is a V-hedra with planar quads, each vertex of  $\mathcal{V}$  can uniquely be associated with one rotational axis orthogonal to the planar vertex star. Then the resulting network of Bennett mechanisms is highly mobile<sup>6</sup>. Finally it should be noted that in this case  $\mathcal{V}$  is a discrete pseudospherical surface [4,15,26].

<sup>6</sup>The degree of the mobility corresponds to the number of rows plus columns of  $\mathcal{V}$  minus one (cf. Sauer [15, Theorem 11.18]).

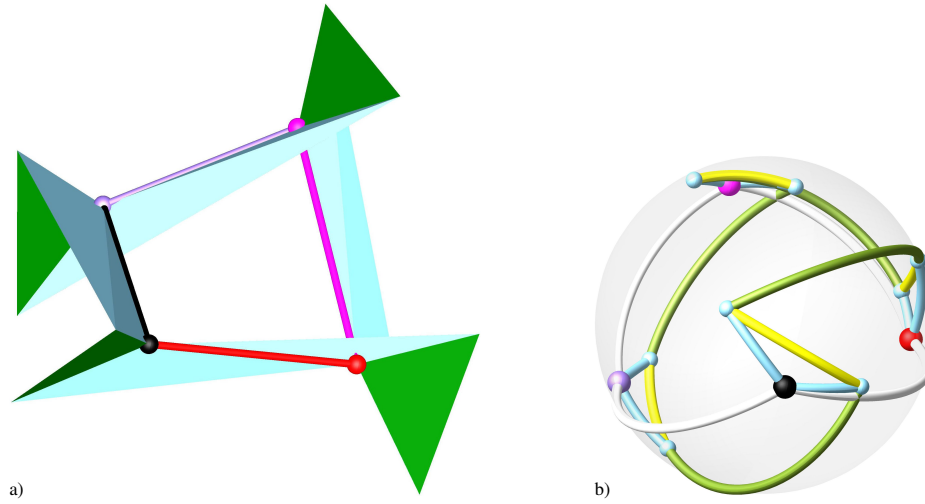


**Fig. 4.** A  $(3 \times 3)$  building block of a V-hedra with skew quads (a) and its spherical image (b). The vertex  $V_i$  and the line-segment  $V_{i-1}V_i$  have the same color, where  $i = 0$  corresponds to black,  $i = 1$  to red,  $i = 2$  to magenta and  $i = 3$  to purple. Note that the illustrations of Figs. 4, 5 and 6 are rendered with respect to the same view. The animations of the mobility of the V-hedra and its spherical image are online available at [https://www.dmg.tuwien.ac.at/nawratil/skew\\_quad\\_spatial.gif](https://www.dmg.tuwien.ac.at/nawratil/skew_quad_spatial.gif) and [https://www.dmg.tuwien.ac.at/nawratil/skew\\_quad\\_spherical.gif](https://www.dmg.tuwien.ac.at/nawratil/skew_quad_spherical.gif), respectively.

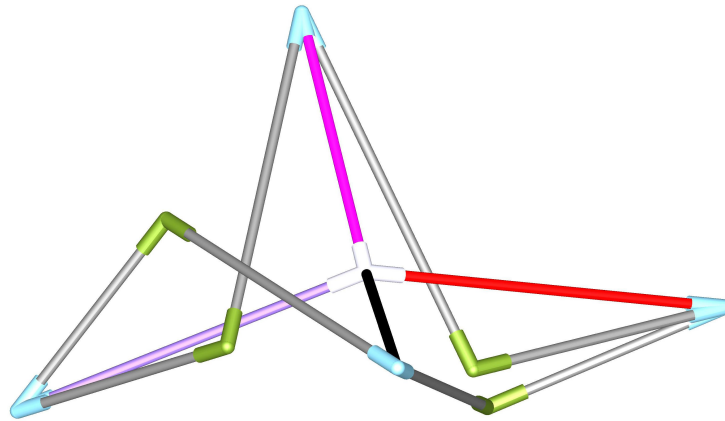


**Fig. 5.** The overconstrained mechanism which results from the reciprocal-parallelism to the  $(3 \times 3)$  building block of a V-hedra with skew quads illustrated in Fig. 4a. The animation of the mobility of this mechanism is online available at [https://www.dmg.tuwien.ac.at/nawratil/skew\\_quad\\_reciprocal.gif](https://www.dmg.tuwien.ac.at/nawratil/skew_quad_reciprocal.gif), where we fixed the length of the black edge, which is parallel to  $V_3V_0$ .

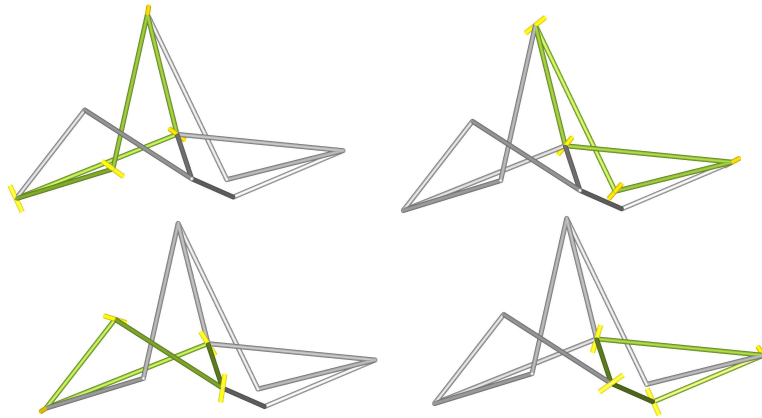


**Fig. 6.** The four Bennett mechanisms associated with the structure illustrated in Fig. 5, where the rotation axes are displayed in yellow.

## 5 Conclusions, open problems and future research

We generalized continuous flexible Kokotsakis belts of the isogonal type by allowing that the faces, which are adjacent to the line-segments of the rigid closed polygon  $p$ , to be skew. In more detail we studied the case where  $p$  is a skew quad as it corresponds to a  $(3 \times 3)$  building block of a V-hedra composed of skew quads, which proves (under consideration of Theorem 3) the existence of continuous flexible SQ surfaces.

Open questions in this context regard the smooth analog of continuous flexible Kokotsakis belts of the isogonal type and of V-hedra with skew quads.

This study at hand is also the starting point towards a full classification of continuous flexible  $(3 \times 3)$  SQ building blocks, which is subject to future research.

**Acknowledgements.** The research is supported by grant F77 (SFB “Advanced Computational Design”, subproject SP7) of the Austrian Science Fund FWF.

## References

1. Kokotsakis, A.: Über bewegliche Polyeder. *Mathematische Annalen* **107**:627–647 (1932)
2. Karpenkov, O.N.: On the flexibility of Kokotsakis meshes. *Geometriae Dedicata* **147**:15–28 (2010)
3. Voss, A.: Über diejenigen Flächen, auf denen geodätische Linien ein konjugiertes System bilden. *Münchener Berichte*, pp. 95–102 (1888)
4. Schief, W.K., Bobenko, A.I., Hoffmann, T.: On the integrability of infinitesimal and finite deformations of polyhedral surfaces. *Discrete Differential Geometry (A.I. Bobenko et al. eds.), Oberwolfach Seminars* **38**:67–93 (2008)
5. Evans, T.A., Lang, R.J., Magleby, S.P., Howell, L.L.: Rigidly foldable origami twists. *Origami<sup>6</sup>, I: Mathematics (K. Miura et al. eds.)*, pp. 119–130, American Mathematical Society (2015)

6. Stachel, H.: A kinematic approach to Kokotsakis meshes. *Computer Aided Geometric Design* **27**:428–437 (2010)
7. Bricard, R.: Mémoire sur la théorie de l’octaèdre articulé. *Journal de Mathématiques pures et appliquées, Liouville* **3**:113–148 (1897)
8. Stachel, H.: Remarks on Bricard’s flexible octahedra of type 3. *Proceedings of the 10th International Conference on Geometry and Graphics (July 28 - Aug. 3, 2002, Kiev/Ukraine)*, **1**:8–12 (2002)
9. Nawratil, G.: Flexible octahedra in the projective extension of the Euclidean 3-space. *Journal for Geometry and Graphics* **14**(2):147–169 (2010)
10. Nawratil, G., Stachel, H.: Composition of spherical four-bar-mechanisms. *New Trends in Mechanisms Science – Analysis & Design* (D. Pisla et al. eds.), pp. 99–106, Springer (2010)
11. Nawratil, G.: Reducible compositions of spherical four-bar linkages with a spherical coupler component. *Mechanism and Machine Theory* **46**(5):725–742 (2011)
12. Nawratil, G.: Reducible compositions of spherical four-bar linkages without a spherical coupler component. *Mechanism and Machine Theory* **49**:87–103 (2012)
13. Izmetiev, I.: Classification of flexible Kokotsakis polyhedra with quadrangular base. *International Mathematics Research Notices* **2017**(3):715–808 (2017)
14. Sauer, R., Graf, H.: Über Flächenverbiegung in Analogie zur Verknickung offener Facettenfläche. *Mathematische Annalen* **105**:499–535 (1931)
15. Sauer, R.: *Differenzgeometrie*. Springer (1970)
16. Sharifmoghaddam, K., Nawratil, G., Rasoulzadeh, A., Tervooren, J.: Using Flexible Trapezoidal Quad-Surfaces for Transformable Design. *Proceedings of the IASS Annual Symposium 2020/21 and the 7th International Conference on Spatial Structures, IASS* (in press)
17. Montagne, N., Douthe, C., Tellier, X., Fivet, C., Baverel, O.: Voss surfaces: a design space for geodesic gridshells. *Journal of the International Association for Shell and Spatial Structures* **61**(206):255–263 (2020)
18. Tachi, T.: Generalization of rigid foldable quadrilateral mesh origami. *Journal of the International Association for Shell and Spatial Structures* **50**(3):173–179 (2009)
19. Tachi, T.: Freeform Rigid-Foldable Structure using Bidirectionally Flat-Foldable Planar Quadrilateral Mesh. *Advances in Architectural Geometry* (C. Ceccato et al. eds.), pp. 87–102, Springer (2010)
20. Feng, F., Dang, X., James, R.D., Plucinsky, P.: The designs and deformations of rigidly and flat-foldable quadrilateral mesh origami. *Journal of the Mechanics and Physics of Solids* **142**:104018 (2020)
21. Dang, X., Feng, F., Plucinsky, P., James, R.D., Duan, H., Wang, J.: Inverse design of deployable origami structures that approximate a general surface. *International Journal of Solids and Structures* **234-235**:111224 (2022)
22. Jiang, C., Wang, H., Inza, V.C., Dellinger, F., Rist, F., Wallner, J., Pottmann, H.: Using isometries for computational design and fabrication. *ACM Transactions on Graphics* **40**(4):42 (2021)
23. Li, Z., Schicho, J.: Classification of angle-symmetric 6R linkages. *Mechanism and Machine Theory* **70**:372–379 (2013)
24. Mitchell, T., Mazurek, A., Hartz, C., Miki, M., Baker, W.: Structural Applications of the Graphic Statics and Static-Kinematic Dualities: Rigid Origami, Self-Centering Cable Nets, and Linkage Meshes. *Proceedings of the IASS Annual Symposium (July 16-20, 2018, Boston/USA), Symposium: Graphic statics*, pp. 1-8(8) (2018)
25. Bennett, G.T.: The skew isogram mechanism. *Proceedings of the London Mathematical Society* **s2-13**(1):151–173 (1914)
26. Wunderlich, W.: Zur Differenzgeometrie der Flächen konstanter negativer Krümmung. *Sitzungsbericht der Österreichischen Akademie der Wissenschaften, Mathem.-Naturw. Klasse IIa* **160**(1-5):39–77 (1951)